The Journal of Physical Chemistry Letters

Letter

pubs.acs.org/JPCL

Stabilization of the Perovskite Phase of Formamidinium Lead Triiodide by Methylammonium, Cs, and/or Rb Doping

Olga A. Syzgantseva,[†] Michael Saliba,[‡] Michael Grätzel,[‡] and Ursula Rothlisberger*[,†]

[†]Laboratory of Computational Chemistry and Biochemistry and [‡]Laboratory of Photonics and Interfaces, Institute of Chemical Sciences and Engineering, École Polytechnique Fédérale de Lausanne, CH-1015 Lausanne, Switzerland

Supporting Information

ABSTRACT: In this work we perform a computational study comparing the influence of monovalent cation substitution by methylammonium (MA^+), cesium (Cs^+), and rubidium (Rb^+) on the properties of formamidinium lead triiodide ($FAPbI_3$)-based perovskites. The relative stability of the desired, photoactive perovskite α phase ("black phase") and the nonphotoactive, nonperovskite δ phase ("yellow phase") is studied as a function of dopant nature, concentration and temperature. Cs^+ and Rb^+ are shown to be more efficient in the stabilization of the perovskite α phase than MA^+. Furthermore, varying the dopant concentration allows changing the relative stability at different temperatures, in particular stabilizing the α phase already at 200 K. Upon Cs^+ or Rb^+ doping, the corresponding onset of the optical spectrum is blue-shifted by 0.1−0.2 eV with respect to pure $FAPbI_3$.

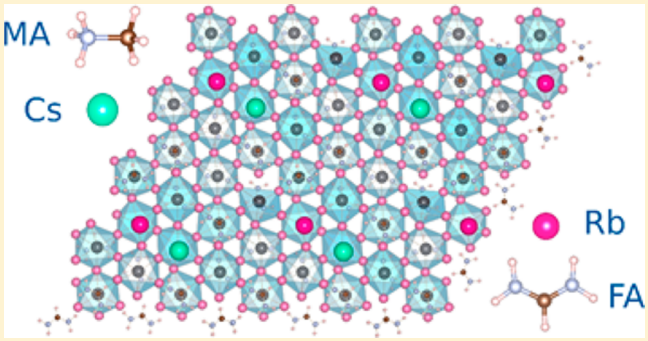

A broad implementation of perovskite solar cells requires an improvement of perovskite light-absorber stability with respect to phase transitions and chemical transformations under operating conditions.[1−3] Indeed, most of the currently proposed materials (ex. $FAPbI_3$, $CsPbI_3$) are not thermodynamically stable in the perovskite phase at room temperature, and special preparation procedures and composition modifications are required for stabilization.[1,2] To this end, it has been proposed to modify the perovskite by cationic or anionic mixing. In particular, recent experimental and theoretical studies suggested mixed Cs−MA, Cs−FA, and MA−FA[4] as alternatives to single-cation perovskite compounds.[4−12] However, this mixing may still entail long-term instability where the new compounds transform into nonperovskite phases which are more stable at room temperature. Additionally, methylammonium (MA)-based perovskites are reported to suffer from chemical decomposition/evaporation of organic cation and halide segregation when operated under full illumination.[13,14] Thus, reducing the amount or even fully replacing MA^+ is desirable. Ideally, a strict control over the phase composition of the light-absorbers should be ensured already at the preparation stage, i.e., the perovskite material should be clean from admixture of nonperovskite phases. For these reasons, it is essential to understand how modifications of the structure and chemical composition impact phase stability and optical characteristics. Indeed, multicomponent perovskite design can enable a creation of stable structures with optimal transport and optical properties.

In this study, we rationalize the effects of MA^+, Cs^+, and Rb^+ doping of $FAPbI_3$ on the stability of the perovskite α phase with respect to the nonperovskite δ phase and on the optical properties. Both $FAPbI_3$ and $CsPbI_3$ form δ phases at room temperature, while the α phase is only stable at higher temperatures.[2,15] For $RbPbI_3$, only a δ phase is known, while an α phase has not been reported.[16] Finally, $MAPbI_3$ exists in several (orthorhombic, tetragonal, and cubic), perovskite phases, while a δ phase has not yet been detected experimentally.[17]

To study the relative stabilization of α with respect to δ phase, we have performed simulations of a series of α and δ structures, in which FA cations were successively substituted by MA^+, Cs^+ or Rb^+ ions, with concentrations ranging from 8.3, 16.7, 25.0, 33.3, 41.7 to 50.0%, that corresponds respectively to $^1/_{12}$ − $^6/_{12}$ dopant cations per unit cell. Structural relaxations including cell parameters were performed for these series of α and δ phase structures (Figure 1). Using a proper band alignment, the energy difference between α and δ structures constitutes a measure of the relative stability of the two phases for a fixed chemical composition at Zero-Kelvin (0K), while the corresponding difference between the average internal energies characterizes the relative phase stability at finite temperature.

In 0 K calculations of pure $FAPbI_3$ and $CsPbI_3$ phases, the δ phase is lower in energy than the α phase, in agreement with experimental observations according to which the low temperature phase of these compounds is a δ phase, while the α phase becomes stable only above 130−160 and 310 °C, respectively.[2,3,6,15]

Received: December 22, 2016
Accepted: February 23, 2017
Published: February 23, 2017

Downloaded via ECOLE POLYTECHNIC FED LAUSANNE on January 28, 2019 at 13:25:01 (UTC).
See https://pubs.acs.org/sharingguidelines for options on how to legitimately share published articles.

ACS Publications © 2017 American Chemical Society

DOI: 10.1021/acs.jpclett.6b03014
J. Phys. Chem. Lett. 2017, 8, 1191−1196

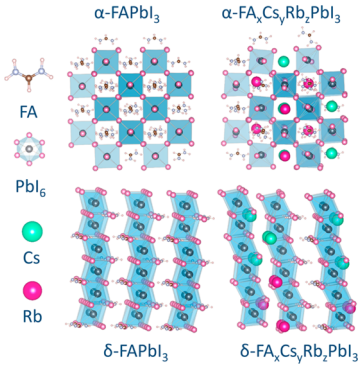

Figure 1. Structures of pure $FAPbI_3$ and mixed $FA_xCs_yRb_zPbI_3$ in α and δ phases.

In fact, at 0 K the calculated energy differences between α and δ phases for pure $FAPbI_3$ and $CsPbI_3$ are 0.20 and 0.18 eV per stoichiometric unit, respectively. Comparison of the analogous energy differences between α and δ phases of the MA^+, Cs^+, or Rb^+ dopant series (Table 1) shows that substitution by any of these cations leads to a monotonic increase of the α phase stabilization as a function of dopant concentration. Furthermore, it turns out that MA^+ is less efficient in the stabilization of the perovskite phase as compared to Cs^+ and Rb^+. In addition, at 0 K Cs^+ provides a slightly better perovskite stabilization at low concentrations (8−17%), while at higher levels of doping (42−50%) Rb^+ becomes more efficient (Table 1).

Even though these trends are evident from (static) 0 K calculations, it is essential to understand how the finite temperature dynamics of the system influences the relative phase stability. Indeed, experimentally it is known that perovskite phases are stable at high temperatures, while the δ phase is preferred at low temperatures. In addition, in the case of MA^+ doped systems, the organic cation can rotate with respect to the Pb−I framework producing a series of local, energetically close lying minima that can be populated at finite temperature. First-principles molecular dynamics simulations of these systems can help to unravel the impact of temperature on phase stability.

To characterize the temperature dependence, the ionic dynamics of each system above was simulated at 200, 400, and 600 K, using Car−Parrinello molecular dynamics (CPMD). The time-averaged relative potential energies of α and δ phases are given in Table 1. In spite of the restrictions due to the rather short simulation lengths and the limited statistics via single MD runs, there are a number of significant trends that emerge. Potential energy curves as a function of time and temperature for fixed concentrations of MA^+ demonstrate that even at 600 K, low MA^+ concentrations do not invert the stabilization order of α and δ phases of $FAPbI_3$ (Figure S1, Supporting Information (SI)). Importantly, the simulations at 600 K allow to observe the rotation of MA cations already at picosecond time scale, suggesting that the lack of stabilization is not related to the hindrance of particular vibrational or rotational modes. Only at 42−50% MA^+ content do the average relative energy values get closer (Table 1). At 200 K, α and δ energy profiles stay well separated for all MA concentrations investigated. This temperature dependence is in line with that observed experimentally.[1,10] The temperature dependence of the internal energy of the system can be used to estimate C_v in the given temperature range, and as a consequence the variation of vibrational entropy. The analysis for MA-doped systems shows a small C_v difference between α and δ phases. It should be mentioned, that other processes occurring at longer time scales, such as possible transformations of methylammonium and/or formamidinium at higher temperatures, should be accounted for separately when assessing the overall stability of mixed system.

The situation is different for Cs^+ and Rb^+. The doping effect for stabilization of the α phase with respect to the δ phase is visible already for small dopant concentrations. For higher dopant concentrations (>25%), the energies of α and δ phases approach each other closely already in a temperature range of 200−400 K. Importantly, at 42−50% of Cs^+ or Rb^+, the energies of α and δ phases approach each other already at 200 K, unlike the case of 50% MA^+ doping. This finding suggests that a particular mixing ratio of Cs^+/Rb^+ and FA^+ cations can provide a thermodynamically stable perovskite phase at or even below room temperature.

With this regard, it is interesting to analyze the stability of mixed perovskite phases with respect to the pure phases. In Table 2, we present the stabilization energies at 0 K with respect to pure α and δ phases. The Cs-doped compounds are stabilized with respect to α-$FAPbI_3$ and high temperature cubic $Pm\bar{3}m$ α-$CsPbI_3$ perovskite structures. In contrast to the Rb-doped systems that are slightly destabilized with respect to the pure α-$FAPbI_3$ and δ-$RbPbI_3$ phases (using the δ phase of $RbPbI_3$ as a reference for the pure compound since no perovskite phase has been reported for this system), this destabilization may be attributed to the stabilization of δ-

Table 1. Stabilization Energies (in eV Per Stoichiometric Unit) of Perovskite Phase with Respect to δ Phase ($\Delta E_{\alpha\delta} = E_\alpha - E_\delta$) upon Doping of $FAPbI_3$ by MA^+, Cs^+, or Rb^+[a]

	MA				Cs				Rb			
conc/T	0	200	400	600	0	200	400	600	0	200	400	600
8%	0.18	0.12	0.13	0.11	0.16	0.11	0.12	0.12	0.18	0.11	0.11	0.11
17%	0.16	0.12	0.12	0.13	0.15	0.10	0.10	0.10	0.16	0.09	0.09	0.07
25%	0.17	0.12	0.13	0.13	0.13	0.08	0.07	0.06	0.14	0.09	0.09	0.07
33%	0.14	0.09	0.09	0.08	0.11	0.05	0.04	0.03	0.12	0.04	0.03	0.02
42%	0.14	0.09	0.08	0.04	0.10	0.02	0.02	−0.01	0.09	0.00	0.00	0.00
50%	0.11	0.06	0.06	0.07	0.11	0.01	0.00	0.02	0.10	0.00	0.01	0.02

[a]The values at 0 K represent the energy difference for the relaxed structures at 0 K. Values for 200−600 K correspond to the difference of the average potential energies of α and δ phases after equilibration (averaged over 1 ps). The standard deviations from the mean energy values varies between 0.01 and 0.03 eV, 0.05 and 0.06 eV, and 0.07 and 0.09 eV for 200, 400, and 600 K temperatures, respectively. Energies were aligned with respect to the position of the Pb_{5d} peak in the density of states of α and δ phases: $\Delta E_{\alpha\delta\text{-corrected}} = \Delta E_{\alpha\delta} - \Delta E_{\alpha\delta_\text{Pb 5d}}$.[8,18]

DOI: 10.1021/acs.jpclett.6b03014
J. Phys. Chem. Lett. 2017, 8, 1191−1196

Table 2. Stabilization/Destabilization of Mixed Cs−FA and Rb−FA Perovskite Phases (in eV Per Stoichiometric Unit) with Respect to Pure α and δ Phases at 0 K[a]

Cs content, %	$E_{\alpha\text{-mix}} - (1-x)E_{\alpha(\mathrm{FA})} - xE_{\alpha(\mathrm{Cs})}$	$E_{\delta\text{-mix}} - (1-x)E_{\delta(\mathrm{FA})} - xE_{\delta(\mathrm{Cs})}$
8%	0.00	0.02
17%	−0.01	0.01
25%	−0.03	0.01
33%	−0.04	0.02
42%	−0.05	0.02
50%	−0.06	0.01
Rb content, %	$E_{\alpha\text{-mix}} - (1-x)E_{\alpha(\mathrm{FA})} - xE_{\delta(\mathrm{Rb})}$	$E_{\delta\text{-mix}} - (1-x)E_{\delta(\mathrm{FA})} - xE_{\delta(\mathrm{Rb})}$
8%	0.02	0.00
17%	0.03	0.01
25%	0.04	0.03
33%	0.04	0.04
42%	0.03	0.05
50%	0.05	0.04

[a]For $RbPbI_3$, the δ-phase is always used as a reference since no perovskite phase has been reported. α-$CsPbI_3$ corresponds to the perfectly cubic Pm-3m phase. For comparison, the mixing entropy contribution $T\Delta S$ even at 600 K does not exceed 0.04 eV/per stoichiometric unit for 50% cation mixing.

$RbPbI_3$ at 0 K. An analysis of the stability of perovskite phases with respect to δ-$FAPbI_3$, δ-$CsPbI_3$, and δ-$RbPbI_3$ phases reveals the perovskite instability at 0K, which is in line with the observed low temperature stability of δ phases. It should be noted that inclusion of the mixing entropy improves the stability of the α phase with respect to all nonperovskite phases. This can be illustrated for example using the formation energies of $FA_{1-x}Rb_xPbI_3$ phase (Figure 2).

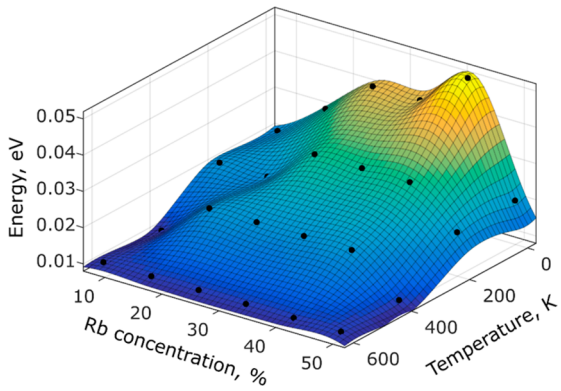

Figure 2. Stabilization of $FA_{1-x}Rb_xPbI_3$ structures with respect to $FAPbI_3$ and $RbPbI_3$ including the mixing entropy contribution.

The increased phase stability of Cs^+ and Rb^+ doped system comes about with only a slight deterioration of the optical properties. The absorption spectra for MA^+, Cs^+, and Rb^+ doped compounds (Figure 3) are similar, even though MA^+ (Figure 3a)-doped compounds provide a slightly better onset. In all cases, the onset of the optical spectra is at maximum blue-shifted by 0.1−0.2 eV (Figure 3). For Cs^+ (Figure 3b) and Rb^+ (Figure 3c), this blue shift increases monotonically with dopant concentration and is more pronounced in the case of Rb^+. These results are in good agreement with experimental findings, according to which Cs and Rb incorporation increases the band gap.[1,9,10]

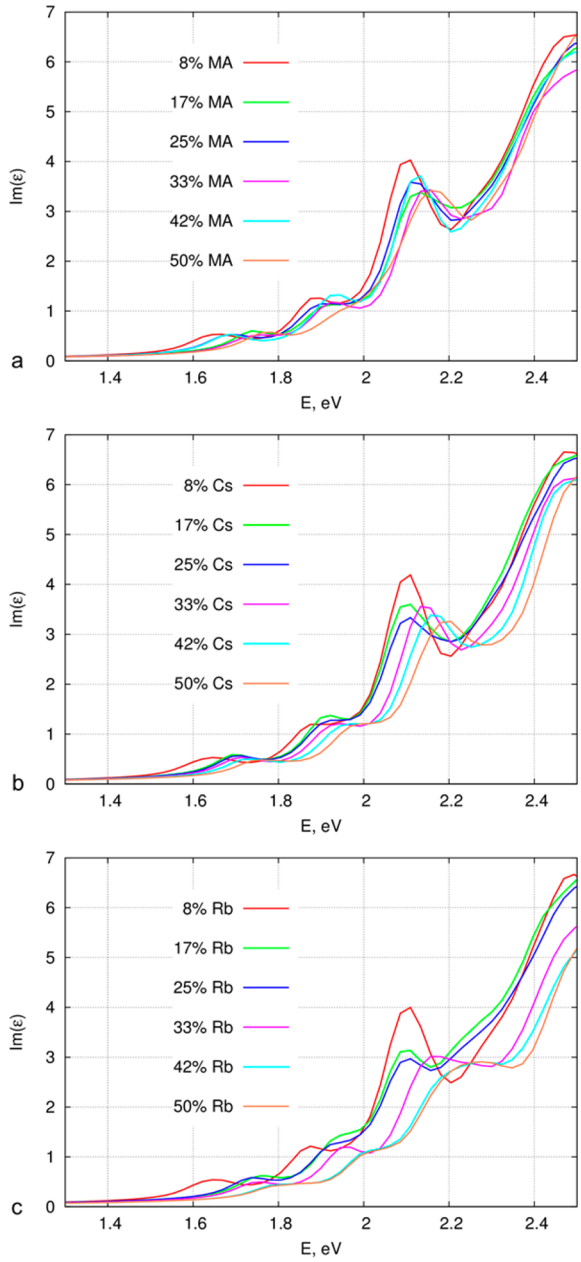

Figure 3. Optical absorption spectra (imaginary part of dielectric function ε) for MA^+ (a), Cs^+ (b), and Rb^+ (c)-doped $FAPbI_3$ structures as a function of dopant concentration.

The fact that Rb^+ at higher concentrations becomes more efficient for the stabilization of the α phase than Cs^+, while at lower concentrations Cs^+ is a more efficient dopant, suggests that the doping by a mixture of Cs^+ and Rb^+ could have a synergetic effect on perovskite stabilization. To verify this hypothesis, we have optimized mixed Cs^+/Rb^+-doped structures with total concentration of admixed cations varying in the range of 25−50%.

At lower dopant concentrations of 25−33%, the presence of Rb^+ does not improve α phase stabilization as compared to the same concentrations of exclusive Cs^+ doping, which is in line with the above observation of higher efficiency of Cs^+ versus Rb^+ at their lower content (Table 3, Figure 4).

On the contrary, at 42−50% of Cs/Rb mixing the presence of Rb allows to achieve an additional 10% stabilization with

DOI: 10.1021/acs.jpclett.6b03014
J. Phys. Chem. Lett. 2017, 8, 1191−1196

Table 3. Stabilization Energies (in eV Per Stoichiometric Unit) of Mixed Perovskite α Phase with Respect to Mixed δ Phase ($\Delta E_{\alpha\delta} = E_\alpha - E_\delta$) for Various Concentrations and Ratios of Cs^+ and Rb^+ in $FAPbI_3$[a]

	Cs+Rb = 25%	Cs+Rb = 33%	Cs+Rb = 42%	Cs+Rb = 50%
% Rb	ΔE	ΔE	ΔE	ΔE
0	0.13	0.11	0.10	0.11
8.3	0.13	0.11	0.09	0.11
16.7	0.13	0.11	0.08	0.10
25.0	0.14	0.12	0.09	0.11
33.3	-	0.12	0.09	0.10
41.7	-	-	0.09	0.10
50.0	-	-	-	0.10

[a]The values represent the energy difference for relaxed structures at 0 K after alignment, with respect to the position of the Pb_{5d} peak in the density of states of α and δ phases: $\Delta E_{\alpha\delta}$-corrected = $\Delta E_{\alpha\delta}$ − $\Delta E_{\alpha\delta}$_Pb_{5d}.[8,18]

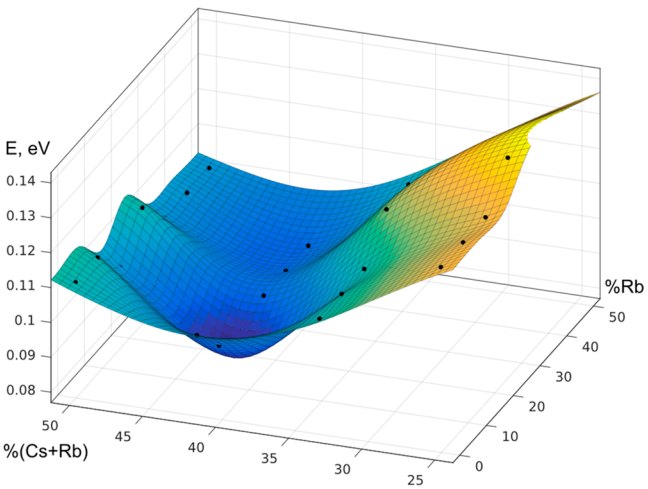

Figure 4. Graphical representation of perovskite phase stabilization upon Cs and Rb mixing into $FAPbI_3$ perovskite phase.

respect to "pure" Cs doping. Simulations of dynamics of these systems at 200−600 K shows that in all cases the α−δ energy difference is close to 0 (−0.01−0.02 eV). Thus, the relative stability is unaffected by temperature and Cs:Rb ratio, suggesting that the phase should be stable above 200 K and that the ratio control over the Cs and Rb concentrations is flexible. For the last series with 50% of dopant we have simulated the optical absorption spectra as a function of Cs/Rb ratio. Figure 5a demonstrates the independence of the absorption spectra on the ratio between Cs and Rb. Hence, in the case of mixed Cs/Rb doping, the shift of the onset depends only on the total concentration of the Cs/Rb type of dopant and is insensitive to its ratio.

Concerning further improvements of the absorption spectra, one would expect that MA^+ doping has less impact than Cs or Rb, as the band gap of $MAPbI_3$ perovskite is closer to that of $FAPbI_3$. To compare the influence of MA^+, Cs^+, and Rb^+ on the absorption spectra in the presence of each other, we simulated perovskite structures with total dopant concentrations of 50% and different ratios of the three cations (Figure 5b). Remarkably, the spectrum of the MA/Rb system has a larger blue shift compared to MA/Cs and MA/Cs/Rb mixtures. Yet the influence of MA on the absorption spectra is minor compared to structures without it (Figure 5b). Consequently, the presence of MA can be avoided in the mixed samples as it is subject to chemical instability and is less efficient for the stabilization of α phase.

Interestingly, following the evolution of the unit cell volumes as a function of Cs/Rb concentration, we notice that the volumes of the α and δ phases approach each other upon an increase of Cs/Rb concentration (Figure 6) within the trigonal $FAPbI_3$ framework. This evolution of cell volumes might have a direct influence on the stabilization of the α phase and requires further detailed investigation. Additionally, for the concentrations of dopant within $FAPbI_3$ higher than 50%, other possible crystallographic structures should be considered, as $FAPbI_3$ has a trigonal symmetry while the reported stable perovskite phase of $CsPbI_3$ is a cubic one.

Finally, it should be noted that our data are in line with recently published experimental results on ternary Cs/MA/FA[10] and quaternary Rb/Cs/MA/FA[1] systems. First, it has been observed both experimentally[1] and theoretically that Rb^+ can stabilize the perovskite phase. Then, experimentally it is shown that various emissive species are present in MAFA films before annealing, while RbCsMAFA films are emissive in a narrower range, suggesting that the initial crystallization conditions for MAFA are less homogeneous than for RbCsMAFA films. Indeed, the X-ray diffraction patterns of unannealed MAFA films contain peaks of the "yellow" phase,

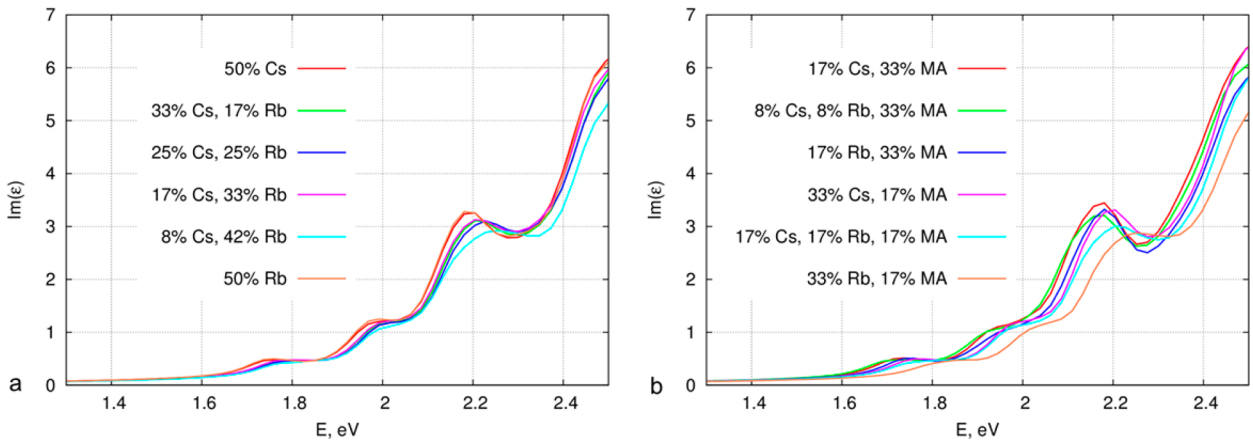

Figure 5. Optical absorption spectra (imaginary part of dielectric function ε) for mixed Cs/Rb and MA/Cs/Rb doped structures as a function of Cs:Rb (a) and MA:Cs:Rb (b) ratios, respectively.

DOI: 10.1021/acs.jpclett.6b03014
J. Phys. Chem. Lett. 2017, 8, 1191−1196

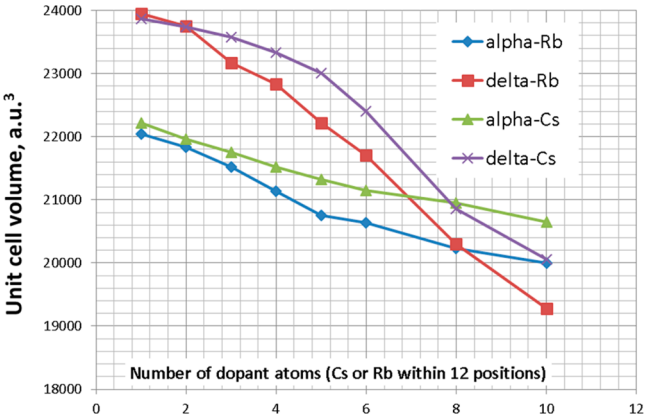

Figure 6. Evolution of the unit cell volumes of α and δ phase as a function of Cs^+ or Rb^+ content (substituted into the initial triclinic $FAPbI_3$ framework).

absent in the case of unannealed RbCsMAFA.[1] The same result is found comparing the CsMAFA and MAFA systems: MAFA compounds have traces of "yellow" $FAPbI_3$ phase seen in the X-ray spectra, while an addition of Cs helps to eliminate it.[10] This is in line with our theoretical observations presented here according to which Rb and Cs doping is able to stabilize the perovskite phase at lower temperatures than MA, thus facilitating the formation of an unannealed precursor close to a final perovskite phase.

In conclusion, our findings suggest that the α perovskite phase of $FAPbI_3$ or $CsPbI_3$ can be stabilized at ambient temperature by choosing an appropriate mixing ratio of monovalent cations, such as Cs or Rb. The onset of the optical spectra of the corresponding systems blue-shifts by 0.1−0.2 eV. Importantly, the demonstrated efficiency of Cs and Rb in stabilizing the perovskite phase paves a way toward replacement of organic cations in lead halide perovskites. Finally, these findings may stimulate the future design of mixed halide perovskites with predefined properties, composed of several major ionic components.

■ COMPUTATIONAL DETAILS

All simulations are performed with density functional theory applying the PBE[19] functional and periodic boundary conditions in all three directions. The structural relaxations, including the cell relaxation, are performed with the Quantum Espresso package,[20] using ultrasoft pseudopotentials[21,22] for all elements, except Rb, for which a norm-conserving pseudopotential was used. Wave function and density cutoffs are 40 and 280 Ry, respectively. An automatically shifted 3 × 3 × 3 k-point grid is used. The Car−Parrinello Molecular Dynamics[23] is accomplished using the CPMD code,[24] with a wave function cutoff of 80 Ry in combination with Trouiller−Martins[25] and Goedecker normconserving[26−28] pseudopotentials for C, H, N and I, Pb, Cs, Rb species, respectively. A time step of 5 au was used with a fictitious electronic mass set to 800 au. The analysis was performed on the trajectories of ∼1.2 ps, after an equilibration phase of ∼1 ps. The temperature in the simulations was set to 200, 400, and 600 K. It was controlled by velocity rescaling with a 10 K tolerance. The initial kinetic energy for each system was set in accordance with the respective temperature to be maintained. The energies of α and δ phases were aligned on the energy of the Pb_{5d} semicore state, as suggested by Meloni and co-workers.[8,18] The optical absorption spectra are simulated with LR-TDDFT using the GPAW[29] program, applying PAW-potentials[30] and 4 × 4 × 4 k-point set. The initial crystal structures are taken from a previous study[8] on mixed Cs-FA perovskite phases. Each structure contained 12 stoichiometric units of $FAPbI_3$ or its substituted analogues.

■ ASSOCIATED CONTENT

Supporting Information

The Supporting Information is available free of charge on the ACS Publications website at DOI: 10.1021/acs.jpclett.6b03014.

Graphs of the evolution of potential energies as a function of dopant nature, concentration, and temperature, tables of stabilization energies without $\Delta E_{\alpha\delta_Pb\ 5d}$ shift, and supercells of α- and δ-phases of $FAPbI_3$ (PDF)

■ AUTHOR INFORMATION

Corresponding Author

*E-mail: ursula.roethlisberger@epfl.ch; Tel: +41 21 69 30321.

ORCID

Olga A. Syzgantseva: 0000-0002-0270-4621

Michael Grätzel: 0000-0002-0068-0195

Notes

The authors declare no competing financial interest.

■ ACKNOWLEDGMENTS

U.R. acknowledges funding from the Swiss National Science Foundation via individual grant No. 200020-146645, the NCCRs MUST and MARVEL, and the NRP70 program. M.S. acknowledges support from the cofunded Marie Skłodowska Curie fellowship, H2020 Grant Agreement No. 665667. M.G. and M.S. acknowledge financial support from the Swiss National Science Foundation (SNSF), the NRP 70 "Energy Turnaround" as well as from SNF-NanoTera and Swiss Federal Office of Energy (SYNERGY). M.G. thanks the King Abdulaziz City for Science and Technology (KACST) for financial support under a joint research project. CSCS Swiss National Supercomputer Center is gratefully acknowledged for providing HPC resources (Projects s672, mr5 and s722).

■ REFERENCES

(1) Saliba, M.; Matsui, T.; Domanski, K.; Seo, J.-Y.; Ummadisingu, A.; Zakeeruddin, S. M.; Correa-Baena, J.-P.; Tress, W. R.; Abate, A.; Hagfeldt, A.; et al. Incorporation of Rubidium Cations into Perovskite Solar Cells Improves Photovoltaic Performance. *Science* **2016**, *354*, 206.

(2) Beal, R. E.; Slotcavage, D. J.; Leijtens, T.; Bowring, A. R.; Belisle, R. A.; Nguyen, W. H.; Burkhard, G. F.; Hoke, E. T.; McGehee, M. D. Cesium Lead Halide Perovskites with Improved Stability for Tandem Solar Cells. *J. Phys. Chem. Lett.* **2016**, *7*, 746−751.

(3) Eperon, G. E.; Paterno, G. M.; Sutton, R. J.; Zampetti, A.; Haghighirad, A. A.; Cacialli, F.; Snaith, H. J. Inorganic Caesium Lead Iodide Perovskite Solar Cells. *J. Mater. Chem. A* **2015**, *3*, 19688.

(4) Pellet, N.; Gao, P.; Gregori, G.; Yang, T.-Y.; Nazeeruddin, M. K.; Maier, J.; Grätzel, M. Mixed-Organic-Cation Perovskite Photovoltaics for Enhanced Solar-Light Harvesting. *Angew. Chem., Int. Ed.* **2014**, *53*, 3151−3157.

(5) Choi, H.; Jeong, J.; Kim, H.-B.; Kim, S.; Walker, B.; Kim, G.-H.; Kim, J. Y. Cesium-Doped Methylammonium Lead Iodide Perovskite Light Absorber for Hybrid Solar Cells. *Nano Energy* **2014**, *7*, 80−85.

(6) Jeon, N. J.; Noh, J. H.; Yang, W. S.; Kim, Y. C.; Ryu, S.; Seo, J.; Seok, S. I. Compositional Engineering of Perovskite Materials for High-Performance Solar Cells. *Nature* **2015**, *517*, 476−480.

DOI: 10.1021/acs.jpclett.6b03014
J. Phys. Chem. Lett. 2017, 8, 1191−1196

(7) Lee, J.-W.; Kim, D.-H.; Kim, H.-S.; Seo, S.-W.; Cho, S. M.; Park, N.-G. Formamidinium and Cesium Hybridization for Photo- and Moisture-Stable Perovskite Solar Cell. *Adv. Energy Mater.* **2015**, *5*, 1501310.
(8) Yi, C.; Luo, J.; Meloni, S.; Boziki, A.; Ashari-Astani, N.; Grätzel, C.; Zakeeruddin, S. M.; Rothlisberger, U.; Grätzel, M. Entropic Stabilization of Mixed A - Cation ABX_3 Metal Halide Perovskites for High Performance Perovskite Solar Cells. *Energy Environ. Sci.* **2016**, *9*, 656−662.
(9) Jacobsson, T. J.; Correa-Baena, J.-P.; Pazoki, M.; Saliba, M.; Schenk, K.; Grätzel, M.; Hagfeldt, A. Exploration of the Compositional Space for Mixed Lead Halogen Perovskites for High Efficiency Solar Cells. *Energy Environ. Sci.* **2016**, *9*, 1706−1724.
(10) Saliba, M.; Matsui, T.; Seo, J.-Y.; Domanski, K.; Correa-Baena, J.-P.; Nazeeruddin, M. K.; Zakeeruddin, S. M.; Tress, W.; Abate, A.; Hagfeldt, A.; et al. Cesium-Containing Triple Cation Perovskite Solar Cells: Improved Stability, Reproducibility and High Efficiency. *Energy Environ. Sci.* **2016**, *9*, 1989−1997.
(11) McMeekin, D. P.; Sadoughi, G.; Rehman, W.; Eperon, G. E.; Saliba, M.; Horantner, M. T.; Haghighirad, A.; Sakai, N.; Korte, L.; Rech, B.; et al. A Mixed-Cation Lead Mixed-Halide Perovskite Absorber for Tandem Solar Cells. *Science* **2016**, *351*, 151−155.
(12) Li, Z.; Yang, M.; Park, J.-S.; Wei, S.-H.; Berry, J.; Zhu, K. Stabilizing Perovskite Structures by Tuning Tolerance Factor: Formation of Formamidinium and Cesium Lead Iodide Solid-State Alloys. *Chem. Mater.* **2016**, *28*, 284.
(13) Frost, J. M.; Butler, K. T.; Brivio, F.; Hendon, C. H.; van Schilfgaarde, M.; Walsh, A. Atomistic Origins of High-Performance in Hybrid Halide Perovskite Solar Cells. *Nano Lett.* **2014**, *14*, 2584−2590.
(14) Deretzis, I.; Alberti, A.; Pellegrino, G.; Smecca, E.; Giannazzo, F.; Sakai, N.; Miyasaka, T.; La Magna, A. Atomistic Origins of $CH_3NH_3PbI_3$ Degradation to PbI_2 in Vacuum. *Appl. Phys. Lett.* **2015**, *106*, 131904.
(15) Binek, A.; Hanusch, F. C.; Docampo, P.; Bein, T. Stabilization of the Trigonal High-Temperature Phase of Formamidinium Lead Iodide. *J. Phys. Chem. Lett.* **2015**, *6*, 1249−1253.
(16) Brgoch, J.; Lehner, A. J.; Chabinyc, M.; Seshadri, R. Ab Initio Calculations of Band Gaps and Absolute Band Positions of Polymorphs of $RbPbI_3$ and $CsPbI_3$: Implications for Main-Group Halide Perovskite Photovoltaics. *J. Phys. Chem. C* **2014**, *118*, 27721−27727.
(17) Ong, K. P.; Goh, T. W.; Xu, Q.; Huan, A. Structural Evolution in Methylammonium Lead Iodide $CH_3NH_3PbI_3$. *J. Phys. Chem. A* **2015**, *119*, 11033−11038.
(18) Meloni, S.; Palermo, G.; Ashari-Astani, N.; Grätzel, M.; Rothlisberger, U. Valence and Conduction Band Tuning in Halide Perovskites for Solar Cell Applications. *J. Mater. Chem. A* **2016**, *4*, 15997−16002.
(19) Perdew, J. P.; Burke, K.; Ernzerhof, M. Generalized Gradient Approximation Made Simple. *Phys. Rev. Lett.* **1996**, *77*, 3865−3868.
(20) Giannozzi, P.; Baroni, S.; Bonini, N.; Calandra, M.; Car, R.; Cavazzoni, C.; Ceresoli, D.; Chiarotti, G. L.; Cococcioni, M.; Dabo, I.; et al. QUANTUM ESPRESSO: a Modular and Open-Source Software Project for Quantum Simulations of Materials. *J. Phys.: Condens. Matter* **2009**, *21*, 395502.
(21) Rappe, A. M.; Rabe, K. M.; Kaxiras, E.; Joannopoulos, J. D. Optimized Pseudopotentials. *Phys. Rev. B: Condens. Matter Mater. Phys.* **1990**, *41*, 1227−1230.
(22) Vanderbilt, D. Soft Self-Consistent Pseudopotentials in a Generalized Eigenvalue Formalism. *Phys. Rev. B: Condens. Matter Mater. Phys.* **1990**, *41*, 7892.
(23) Car, R.; Parrinello, M. Unified Approach for Molecular Dynamics and Density-Functional Theory. *Phys. Rev. Lett.* **1985**, *55*, 2471−2474.
(24) CPMD, http://www.cpmd.org/; Copyright IBM Corp 1990−2015, Copyright MPI für Festkörperforschung Stuttgart 1997−2001.
(25) Troullier, N.; Martins, J. L. Efficient Pseudopotentials for Plane-Wave Calculations. *Phys. Rev. B: Condens. Matter Mater. Phys.* **1991**, *43*, 1993.
(26) Goedecker, S.; Teter, M.; Hutter, J. Separable Dual-Space Gaussian Pseudopotentials. *Phys. Rev. B: Condens. Matter Mater. Phys.* **1996**, *54*, 1703.
(27) Hartwigsen, C.; Goedecker, S.; Hutter, J. Relativistic Separable Dual-Space Gaussian Pseudopotentials from H to Rn. *Phys. Rev. B: Condens. Matter Mater. Phys.* **1998**, *58*, 3641.
(28) Krack, M. Pseudopotentials for H to Kr Optimized for Gradient-Corrected Exchange-Correlation Functionals. *Theor. Chem. Acc.* **2005**, *114*, 145.
(29) Enkovaara, J.; Rostgaard, C.; Mortensen, J. J.; Chen, J.; Dulak, M.; Ferrighi, L.; Gavnholt, J.; Glinsvad, C.; Haikola, V.; Hansen, H. A.; et al. Electronic Structure Calculations with GPAW: a Real-Space Implementation of the Projector Augmented-Wave Method. *J. Phys.: Condens. Matter* **2010**, *22*, 253202.
(30) Blochl, P. E. Projector Augmented-Wave Method. *Phys. Rev. B: Condens. Matter Mater. Phys.* **1994**, *50*, 17953−17979.

DOI: 10.1021/acs.jpclett.6b03014
J. Phys. Chem. Lett. 2017, 8, 1191−1196